

A Comprehensive Study of Fracture Toughness Determination from Conventional and Unconventional Methods

K. Bhattacharyya

*Department of Mechanical Engineering, Netaji Subhash Engineering College, Kolkata - 700 152, India
E-mail: bhattacharyyakushal3@gmail.com*

ABSTRACT

In this work fracture toughness is determined by the Toughness model; Critical Stress-Strain Model and Energy release rate model using unconventional test method referred to as Spherical Indentation test (SIT) to reduce the large and costly experimental set up as required in Conventional Fracture Toughness Test. The toughness model correlates the indentation energy to fracture with fracture toughness, Critical Stress-Strain Model assumes that the critical fracture toughness is equal to the critical plastic work done by the material when a crack tends to propagate and as per the Energy release rate model, indentation depth is given by loading-unloading cycles. The unloading slope which is elastic provides the reduced Young's Modulus of the material from each unloading cycle which reflects the occurrence of damage in the material. For the determination of contact radius at different indentation points, finite element analysis is performed using the material data obtained from the tensile test result obtained from the previous work of the author. Conventional method using the Compact Tension (CT) and Three-Point Bending (TPB) specimens for the same material is used to determine the fracture toughness and compared with the above-described model.

Keywords: Fracture toughness; Spherical indentation test (SIT); TPB specimen; CT specimen

1. INTRODUCTION

Material resistance to crack growth which is coined as fracture toughness serves as an important material property, in accessing the structural integrity of the material. Established fracture toughness tests like the J_{IC} test of Compact Tension (CT) or Three-Point Bending (TPB) specimen use the destructive testing procedure. The test procedure, followed, complicated fatigue pre-cracking and needs sophisticated machines in determining the crack growth with the increase in load and therefore cannot be used in in-service structures like reactor pressure vessels (RPV). Transferability of fracture toughness from laboratory specimens to a structure is an issue of extensive research during the last few decades due to the effect of constraint loss. Several researchers tried to address the effect of constraint loss through different models¹⁻³. Spherical Indentation Test (SIT) is free from the above-mentioned complexities and is quite successful in predicting the uniaxial testing properties⁴⁻⁵. But when it comes to the determination of fracture toughness through SIT, it lacks the requirement of formation of microcracks beneath the indentation which is developed from the fatigue crack in the case of CT and TPB specimen. There is very limited research work on the prediction of fracture and damage mechanisms taking place under compressive load. The implementation

of Shear Damage⁶ in Gurson, Tvergaard, and Needleman's damage model (GTN model) establishes the effect of reduced Effective Young's Modulus due to the effect of void nucleation, micro void coalescence which ultimately affects the damage evaluation and prediction. The application of shear damage in the GTN model can be extended in SIT, as shear failure is considered to be the major factor in the indentation process. Several researchers⁷⁻¹¹ tried to co-relate the fracture toughness predicted from indentation with that of the established procedure based on different assumptions. A direct comparison for the determination of fracture toughness from conventional and Unconventional methods like (SIT) is not available in the literature at least for RPV material therefore it motivates the author to work on this specified area. The author uses the Toughness model, Critical Stress-Strain Model, and Energy release rate model to study the results of SIT and predicts the fracture toughness for the RPV material and compared with the existing conventional method ASTM E-1820.

The study reflects a matching trend of Fracture Toughness obtained from the conventional method (ASTM E-1820), with that of compact tension (CT) specimen using the Critical Stress-Strain Model and a matching trend is observed for the Three-Point Bending specimen using the Energy release rate model. The toughness model reflects a poor matching trend with the results of both the conventional specimens. Therefore it can be predicted from the study that SIT can be an alternative process for the determination of fracture toughness by either

E_{ind} is the Young's Modulus of the material of the Indenter

$$J_{IC} = W_p \quad (11)$$

The model assumes that the critical fracture toughness is equal to the critical plastic work done by the material when a crack tends to propagate as shown in Equation 11. Therefore K_{IC} is predicted with the help of Equation 12.

$$K_{IC} = \sqrt{\frac{E}{1-\nu^2}} J_{IC} \quad (12)$$

3.3 Energy Release Rate Model¹³

As per the model, indentation depth is given by 8 loading-unloading cycles. The unloading slope which is elastic provides the reduced Young's Modulus of the material from each unloading cycle which reflects the occurrence of damage in the material. The damage variable could be calculated by equation 13

$$D = 1 - \frac{E_F}{E_0} \quad (13)$$

Where,

D=damage variable. D=0 indicates no damage as the compressive load is given the Young's Modulus of the material decreases which reflects that damage is taking place in the material. When D reaches 1 it indicates fracture occurs¹⁴.

E_F is the reduced Young's Modulus for each loading cycle

E_0 = Young's Modulus of virgin material

Strain energy for each unloading cycle can be calculated from the area of each unloading cycle by the following equation 14.

$$U_D^{(i)} = \frac{1}{2} P_{max}^{(i)} \left(h_{max}^{(i)} - h_p^{(i)} - \frac{P_{max}^{(i)}}{S_0^{(i)}} \right) \quad (14)$$

Where,

U_D =strain energy

(i) =ith cycle

S_0 =Unloading slope

P_{max} =Maximum load at that cycle

h_p =Plastic depth of an indentation in mm at that cycle

h_{max} =Maximum depth of an indentation in mm at that cycle

As shown in fig.1

$$h_r = h - h_p \quad (15)$$

h_r =Depth of the specimen after elastic recovery.

The area of crack growth for each cycle is given by equation 16.

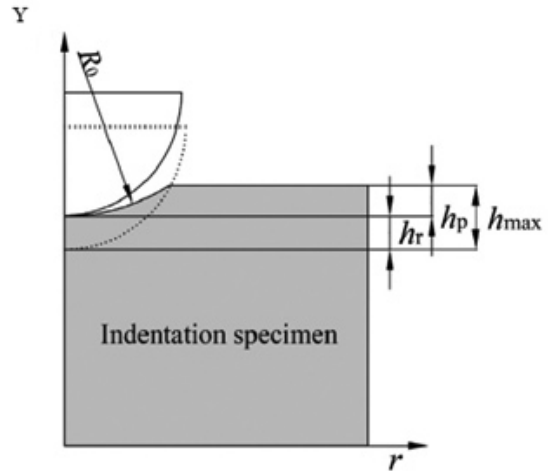


Figure 1. Geometry of the specimen after Indentation.

$$A_{eq}^{(i)} = \pi a_{eff}^2 D^{(i)} \quad (16)$$

Where,

$$a_{eff} = \sqrt{\frac{h_r R R_0}{R_0 - R}} \quad (17)$$

Where,

R=radius of Indenter

$$R_0 = \frac{h_p^2 + (2h_{max}R - h_{max}^2)}{2h_p} \quad (18)$$

As R_0 is known from equation 18 a_{eff} can be calculated from equation 17. To calculate the equivalent crack area from equation 16 Damage variable has to be calculated from each cycle from 13.

Once E_{EFF} is calculated from equation (19) the value of Damage is known and we could plot A_{eq} versus U_D for the total number of cycles. Now a straight line is fitted from the available data.

$$E_{eff} = \frac{1 - \nu^2}{2 \sqrt{\frac{h_r R R_0}{R_0 - R}} \frac{(1 - \nu^2)}{S} E_{ind}} \quad (19)$$

From the straight line fitted we could be able to calculate J_{SIT} from equation 20

$$J_{SIT} = \frac{dU_D}{dA_{eq}} \quad (20)$$

Due to compressive load during indentation shear stress is the dominating phenomenon of fracture therefore energy release rate can be correlated with the mode II fracture test with the help of Equation (21).

$$K_{IIC} = \sqrt{\frac{E_0}{1-\nu^2}} J_{SIT} \tag{21}$$

$$K_{IC} = \frac{K_{IIC}}{\alpha} \tag{22}$$

α is the stress ratio of maximum shear stress ζ_{max} to maximum normal stress σ_{max} and is taken as 0.35^{14,15}

4. EXPERIMENTS

4.1 Tensile Test

The tensile test is performed as per ASTM standard E8 using Instron 8801 as shown in Fig. 2 using a computer-controlled Universal Testing Machine (INSTRON8801) with 100 KN grip capacity.. The tensile tests is done under displacement control mode with a ramp rate corresponding to the displacement rate of .003 mm/min. An axial extensometer of 12.5 mm gauge length which is capable of measuring up to 40% strain was kept attached to the specimen along the gauge length for the test. The test program was controlled by using tensile testing software (Blue Hill). The data acquisition rate was 20 per second.



Figure 2. The tensile test setup.

4.2 Fatigue Pre-cracking

Fatigue pre-cracking of the TPB and CT specimens is performed at room temperature as per ASTM standard E 647 using da/dN software. The crack lengths were measured by a compliance technique using a COD gauge of 10mm gauge length.

4.3 Fracture Test for TPB and CT Specimen

J-Integral of TPB and CT specimens was carried out using J_{IC} software using INSTRON 8801 following ASTM E813 as shown in Fig.3 and Fig.4



Figure 3. Experimental arrangement for ambient temperature J_{IC} tests for TPB Specimen.



Figure 4. Experimental arrangement for ambient temperature J_{IC} tests for CT Specimen.

- | | | |
|-----------------|---------------|-------------------------|
| 1.Top roller | 4. COD Gauge | 9.Tensile Specimen Grip |
| 2.Bottom roller | 7.Pull Road | 10.Tensile Specimen |
| 3.TPB specimen | 8.Lock nut | 11.Extensometer |
| 13=CT specimen | 14= COD Gauge | |

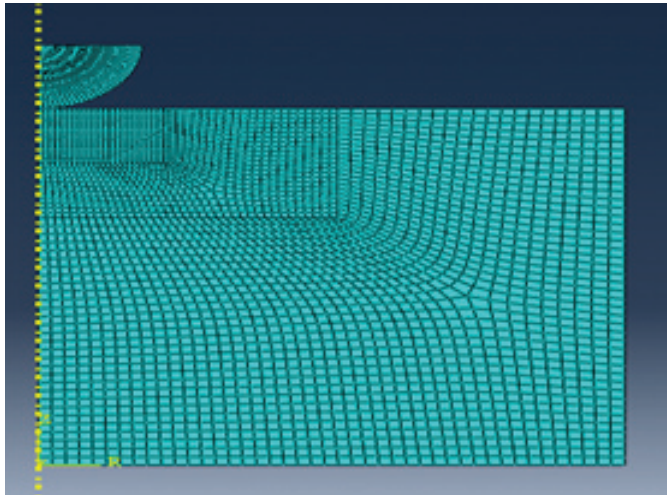
4.4 Spherical Indentation Test

Spherical Indentation test is performed with the help of tungsten carbide indenter having Young's Modulus 710 GPa and Poisson's ratio 0.23. The dimension of the Specimens is 10 ×10 ×50 mm blocks and the radius of the indenter is 0.38 mm. Different typesof mesh sandpapers are used to prepare the indentation surface, then polished with diamond spray. Stress-Strain Microprobe System, (B4000) is used as the indent equipment. The depth of indentation was measured using a high-resolution depth sensor The indentation is carried out in displacement control mode.

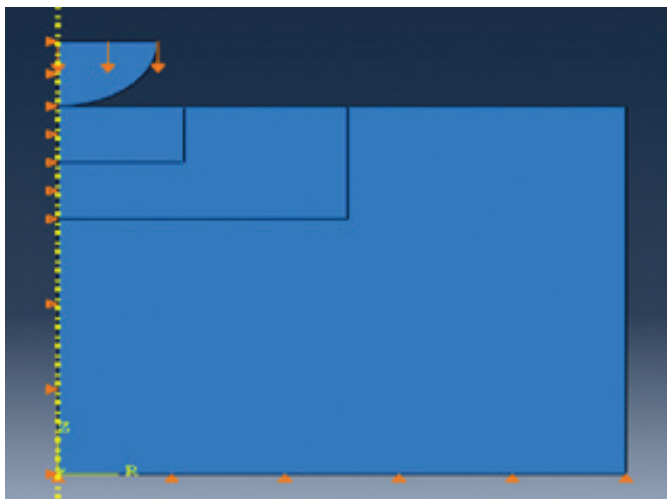
4.5 Finite Element Analysis

Finite element analysis is carried out to calculate the contact radius of the indenter with the specimen 2-Dimensional FE is performed using Abacus 6.13. As the specimen and indenter are cylindrical therefore, axis-symmetric analysis is performed and the element taken is a linear quadrilateral, type CAX4R. The indenter is considered as an elastic element with Young's modulus and poisson's ratio taken as that of SIT. The specimen is taken as Elasto-plastic material the Young's Modulus, Poisson's ratio, and stress versus plastic strain property are taken from the stress-strain diagram of the material. Axis symmetric boundary condition is provided on one side of the specimen and the bottom of the specimen is fixed as shown in Fig. 5(a) & Fig. 5(b)

The indenter is taken as a Master surface and the specimen is taken as a slave surfaced and the coefficient of friction is taken as 0.2 between the indenter and the specimen. The element size is taken as 0.02 mm near the contact portion. The displacement boundary condition is provided on the top of the indenter and the displacement is given 0.2R in the step of 0.01 which generates a plastic strain of 12% as observed. Large



(a)



(b)

Figure 5. (a) Mesh distribution and (b) Boundary Condition.

deformation theory is used to replicate the large strain effect. Full Newton Rapson with reduced integration is performed in the analysis.

5. RESULTS AND DISCUSSIONS

5.1 Tensile Test Property

The stress-strain plot of the material at room temperature is shown in Fig. 6. The Young's Modulus is calculated as 200 GPa and Poisson's Ratio as 0.3. The result reflects the similar unique nature of the tensile test data for the same material done by the previous researchers.¹⁶

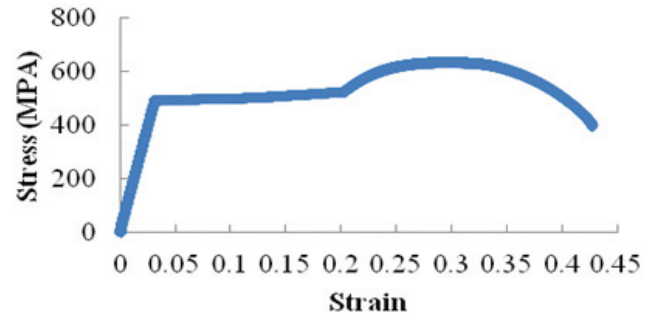


Figure 6. Stress-Strain diagram obtained from tensile test.

5.2 Calculation with the Help of the Toughness Model

From the FE analysis, it is clear that the considered RPV material reflects a pile-up form as shown in Fig. 7. The depth of indentation is given as $0.2 \times \text{Radius of indenter}$ which is equal to 0.076 and is considered as the critical radius h_c . At that indentation depth, the reaction force on the indenter is considered as the applied load which is equal to 310.48 N. The contact area a_c at the critical depth is calculated as 0.000232 m^2 from FE analysis. P_m is calculated as per Equation (2) and is found as 184 Pa. W_{IEF} is calculated as per Equation (1) and ultimately K_{IC} is calculated as 744.5 $\text{MPa}\sqrt{\text{m}}$ from Equation (5).

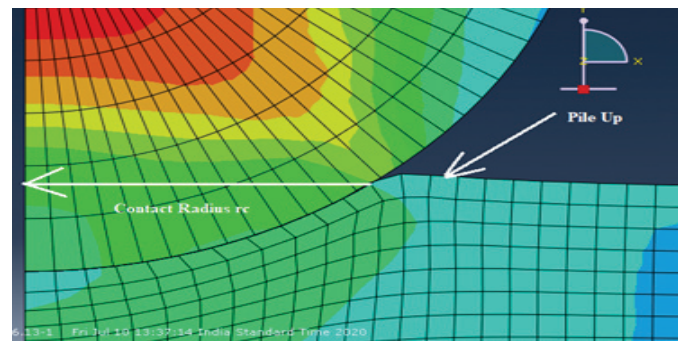


Figure 7. FE result showing pile up form at maximum indentation point.

5.3 Calculation with the help of the Critical Stress-Strain Model

The stress-strain curve predicted from SIT as per equations 7 and 8 is shown in Fig. 8. The curve is fitted by a power-law curve as shown in Fig. 8.

$$y = 20231x^{1.1821} \quad (23)$$

$$Area = \int_0^{h_c} y dx = 2023 \int_0^{0.123} x^{1.1821} dx = 95.768 \text{ mm}^2 \quad (24)$$

This $\left(\frac{dW}{dV}\right)_C$ is calculated from the area under the curve by integrating equation 23. Therefore W_p is calculated from equation 6 and K_{IC} is calculated as 313.84 MPa√m from equations 11 and 12.

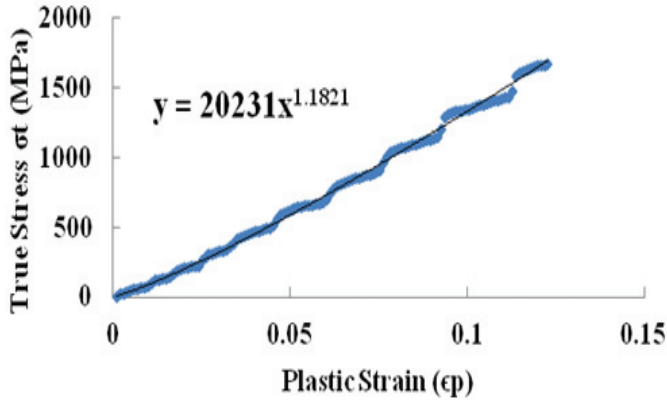


Figure 8. True stress versus Plastic Strain from SIT.

5.4 Calculation with the Help of the Energy Release Rate Model

The strain energy is calculated for each cycle using equation 14 from the loading-unloading curve obtained from SIT as shown in Fig. 9. The E_{EFF} is calculated with the help of Equation (19). Then the damage variable D is calculated with the help of equation 13 as shown in Fig. 10.

Then A_{eq} is calculated for each cycle using equations 16 and 17. Then J_{SIT} as per equation 20 as shown in Fig. 11. The value of K_{IC} is predicted as 391.54 using Equations 20, 21, and 22.

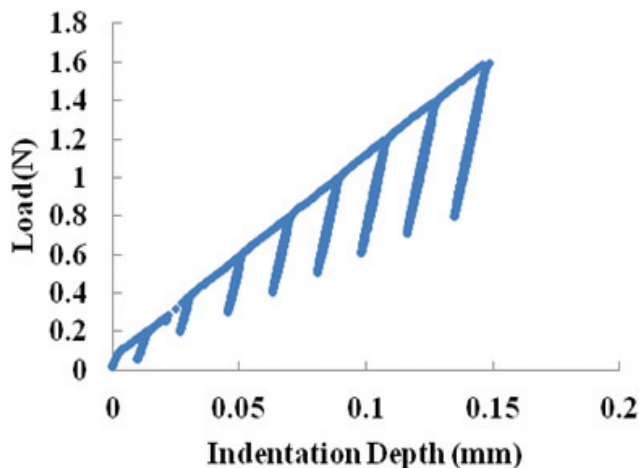


Figure 9. Loading Unloading curve versus Depth of Indentation.

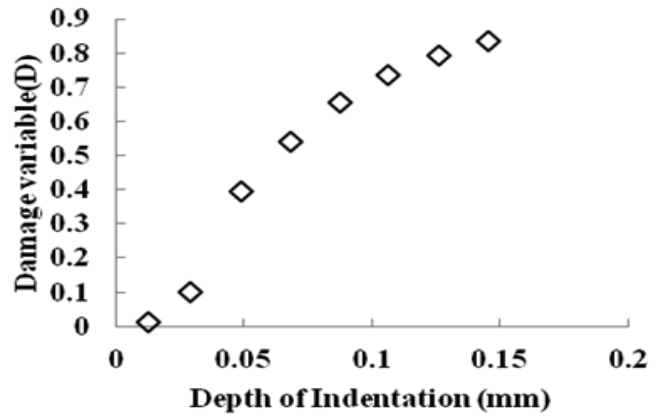


Figure 10. Damage Variable versus Indentation Depth

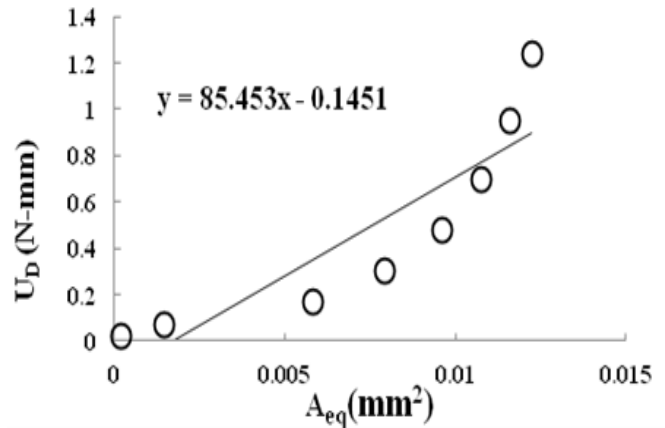


Figure 11. U_D versus A_{eq} for predicting J_{SIT} .

5.5 K_{JC} Predicted from Conventional Compact Tension and Three-Point Bending Specimen

The J versus crack extension obtained for CT and TPB specimens is shown in Fig. 12 and Fig. 13. According to ASTM E1820, crack growth is monitored throughout the test. Extrusion lines are drawn at crack extension 0.15 mm and 1.5 mm. The lines have a slope of $M\sigma_Y$, where σ_Y is the flow stress which is defined as the average yield stress and tensile strength of the material. The yield strength for the referred material is 488 MPa and tensile strength 628 MPa as obtained from the tensile test. The slope of the extrusion line is taken to represent the component of crack extension due to crack blunting as opposed to ductile tearing. The value of M is taken as 2. All data that fall within the exclusion limit are fitted to a power-law expression as shown in Equation (25).

$$J = C_1 (\Delta a)^{C_2} \quad (25)$$

Table 2. The value of the power-law constants derived from experimental J-R curve

Specimens	C_1	C_2
CT	620.44	0.7699
TPB	845.00	0.5254

Table 2 provides the value of the constants for CT and TPB specimens. The J_{IC} is determined as the interaction between the

curve formed with the equation 25 and 0.2 mm offset line. The J_{IC} value obtained for the CT specimen is observed as 400 kJ/m² as shown in Fig.12 and the J_{IC} value obtained for the TPB specimen is observed as 800 kJ/m² as shown in Fig.13. Once J_{IC} is determined K_{JC} can be predicted from Equation 26.

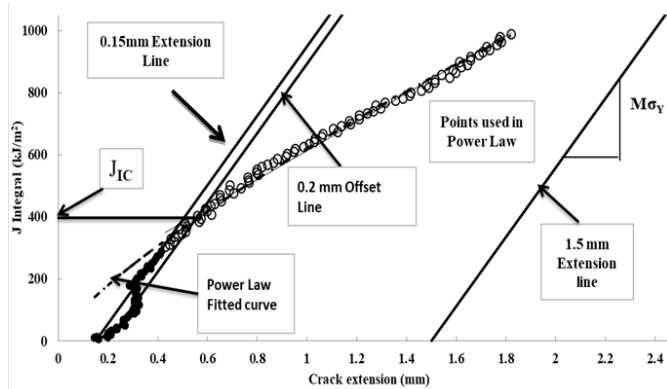


Figure 12. J-R curve for CT specimen.

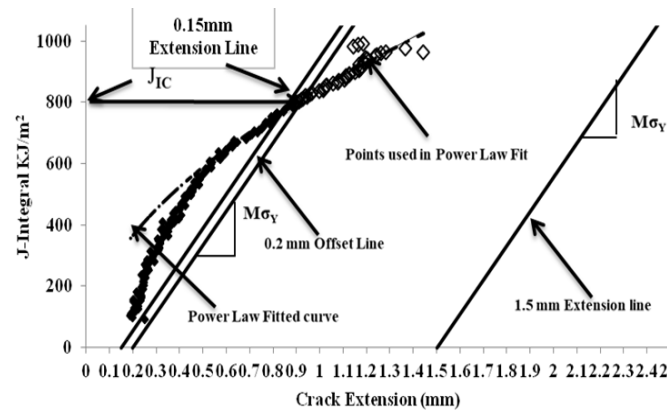


Figure 13. J-R curve for TPB specimen.

$$K_{JC} = \sqrt{\frac{J_{IC} E'}{1 - \nu^2}} \quad (26)$$

The K_{JC} obtained with the help of three different models using SIT and from conventional procedure using CT and TPB specimens for the RPV material are given in table 3.

It is observed that the result predicted by the CSS model matches well with that of the CT specimen result and the ERR model matches that TPB specimen. Due to different geometry between CT and TPB specimen which ultimately affects the loading and stress pattern, there is a difference in K_{JC} value calculated from CT and TPB specimen for the referred material¹⁷. Therefore the result obtained from SIT using CSS model is supported by the results obtained using CT specimen from conventional test and the results from SIT using ERR model is supported by the results obtained using TPB specimen from the conventional test for the RPV material 20MnMoNi55 steel. The fracture toughness predicted from conventional test results differs due to the effect of geometry and loading pattern for the same material so do the SIT test results vary for CSS and ERR models due to the difference in the methodology and physics considered for calculating the fracture toughness data for the same material.

Table 3. K_{JC} values predicted from Conventional and SIT

The model used in SIT	K_{JC} values (MPa√m)
Toughness model	744.5
Critical Stress-Strain Model	313.84
Energy release rate model	391.5455
Conventional Test	
Compact Tension Specimen	296.4997
Three-Point Bending Specimen	419.3139

6. CONCLUSION

The result predicted from SIT shows different values for a different model but the result obtained from the CSS model reflects more or less a matching trend with that of CT specimen and the same is observed for ERR with that of TPB specimen. The fracture toughness predicted from conventional test results differs due to the effect of geometry and loading pattern for the same material so do the SIT test results vary for different models used due to the difference in the methodology and physics considered for calculating the fracture toughness data for the same material. But from this work, two affirmative conclusions can be predicted.

- The toughness model should not be an acceptable methodology for calculating fracture toughness from SIT.
- For the requirement of determination of fracture toughness of the reactor pressure vessel in the working condition, SIT can be a useful alternative for non-destructive test procedures.

Among CSS and ERR the best model to predict fracture toughness is yet to be done by comparing the fracture toughness obtained from conventional method and SIT using them for a variety of materials then only a proper conclusion can be asessed.

REFERENCES

1. Claudio, Ruggieri; Xiaosheng, Gao; H. Dodds Jr, Robert. Transferability of elastic-plastic fracture toughness using the Weibull stress approach: significance of parameter calibration. *Eng. Fract. Mech.*, 2000, **67**, 101-117. doi:10.1016/S0013-7944 (00)00052-7.
2. Bhattacharyya, K.; Acharyya, S.K.; Chattopadhyay, J. & Dhar, S. Study of constraint effect on reference temperature (T₀) of reactor pressure vessel material (20mnmoni55 Steel) in the ductile to Brittle Transition Region. *Procedia Eng.*, 2014, **86**, 264-271. doi:10.1016/j.proeng.2014.11.037
3. Xiaosheng, Ga; Robert, H & Dodds Jr. An engineering approach to assess constraint effects on cleavage fracture toughness. *Eng. Fract. Mech.*, 2001, **68**,

- 263-283.
doi:10.1016/S0013-7944(00)00102-8.
4. Yingzhi, Li; Paul, Stevens; Mingcheng, Sun; Chaoqun, Zhang & Wei, Wang. Improvement of predicting mechanical properties from spherical indentation test. *Int. J. Mech. Sci.*, 2016, **117**:182–96. doi:10.1016/j.ijmecsci.2016.08.019.
 5. Chen, H; Cai, L-X & Bao, C . Equivalent-energy indentation method to predict the tensile properties of light alloys. *Mater. Des.*, 2019, **162**, 322–30. doi:10.1016/j.matdes.2018.11.058
 6. Nahshon, K. & Hutchinson, J.W. Modification of the Gurson Model for shear failure. *European J. Mech. A/Solids*, 2008, **27**, 1–17. doi:10.1016/j.euromechsol.2007.08.002.
 7. Min, He; Fuguo, Li; Jun, Cai & Bo, Chen . An indentation technique for estimating the energy density as fracture toughness with berkovich indenter for ductile bulk materials. *Theor. Appl. Fract. Mech.*, 2011, **56**(2), 104–11. doi:10.1016/j.tafmec.2011.10.006.
 8. Jeon, S.W.; Lee, K.W.; Kim, J.Y.; Kim, W.J.; Park, C.P. & Kwon, D. Estimation of fracture toughness of metallic materials using instrumented Indentation: Critical indentation stress and strain model. *Exp. Mech.*, 2017, **57**, 1013–1025. doi:10.1007/s11340-016-0226-2
 9. Li, J; Li, F; He, M; Xue, F; Zhang, M & Wang, C. Indentation technique for estimating the fracture toughness of 7050 aluminium alloy with the berkovich indenter. *Mater. Des.*, 2012, **40**, 176–184. doi:10.1016/j.matdes.2012.03.054.
 10. Li, J; Li, F; Ma, X; Wang, Q; Dong, J & Yuan, Z. A strain-dependent ductile damage model and its application in the derivation of fracture toughness by micro-indentation. *Mater. Des.*, 2015, **67**, 623–30. doi:10.1016/j.matdes.2014.11.010
 11. Xue, F.M.; Li, F.G.; Li, J & He, M. Strain energy density method for estimating fracture toughness from indentation test of 0Cr12Mn5Ni4Mo3Al steel with berkovich indenter. *Theor. Appl. Fract. Mech.*, 2012, **61**(1), 66–72. doi:10.1016/j.tafmec.2012.08.008.
 12. Haggag, Fahmy M.; Byun, Thak-Sang; Hong, J.H.; Miraglia, P.Q. & Linga Murty, K. Indentation-energy-to-fracture (IEF) parameter for characterization of DBTT in carbon steels using non destructive automated ball indentation (ABI) technique. *Scr. Mater.*, 1998, **38**(4), 645–51 .
 13. Zhang, T.; Wang, S. & Wang, W . A unified energy release rate based model to determine the fracture toughness of ductile metals from unnotched specimens. *Int. J. Mech. Sci.*, 2019, **150**, 35–50. doi:10.1016/j.ijmecsci.2018.10.022
 14. Bonora, N. A Nonlinear CDM Model for ductile failure. *Eng. Fract. Mech.*, 1997, **58**, 11–28. doi:10.1016/S0013-7944(97)00074-X.
 15. Kim Y, *et.al* . Numerical simulation of cup-cone fracture in a round tensile bar. In ASME 2008 Pressure Vessels and Piping Conference. ASME, 2008. pp. 53–60 .
 16. Bhowmik, S.; Chattopadhyaya, A.; Bose, T.; Acharyya, S.K.; Chattopadhyay, J. & Dhar, S. Estimation of fracture toughness of 20MnMoNi55 steel in the ductile to brittle transition region using master curve method. *Nuc. Eng. Des.* 2011, **241**(8), 2831-2838. doi: 10.1016/j.nucengdes.2011.05.033
 17. Bhattacharyy, K.; Acharyya, S.; Dhar, S. & Chattopadhyay, J. *J. Failure Anal. Prev.* s2018/10. doi:10.1007/s11668-018-0549-7

CONTRIBUTOR

Dr Kushal Bhattacharyya received his PhD (Mechanical engineering) from Jadavpur University 2019 and obtained Masters in Mechanical Engineering and Bachelor in Mechanical Engineering from the same university. He has been working as Assistant Professor in Netaji Subhash Engineering College, Kolkata (Techno India Group College) in Mechanical Engineering Department from 2014. He has been working on Computational and Experimental Fracture Mechanics of Reactor Pressure Vessel Material from 2012 and has 8 National and International Publication along with 2 Book Chapters in this field.